INTERNATIONAL JOURNAL FOR NUMERICAL METHODS IN BIOMEDICAL ENGINEERING
Int. J. Numer. Meth. Biomed. Engng. 2010; **26**:1586–1595
Published online 13 March 2009 in Wiley Online Library (wileyonlinelibrary.com). DOI: 10.1002/cnm.1240
COMMUNICATIONS IN NUMERICAL METHODS IN ENGINEERING

Analytical sensitivity of interpolatory quadrature in force-based frame elements

M. H. Scott*,† and O. M. Hamutçuoğlu

School of Civil and Construction Engineering, Oregon State University, 220 Owen Hall, Corvallis, OR 97331, U.S.A.

SUMMARY

Recent literature shows the choice of an integration method in the state determination of force-based frame finite elements has a significant influence on the computed element response. To assess the modeling uncertainty associated with integration methods in force-based elements, analytical sensitivity of one-dimensional interpolatory quadrature is developed via direct differentiation of the governing Vandermonde equations. Comparisons with finite difference calculations show that the combination of the Vandermonde equation sensitivity with equations that govern force-based element response sensitivity leads to an accurate approach to stand-alone response sensitivity analysis. Consistent with previous findings for material, load, and geometric parameters in finite element response sensitivity analysis, sensitivity with respect to parameters associated with the integration method in force-based elements improves the efficiency of gradient-based algorithms where the locations and/or weights of the integration method are treated as uncertain random variables. Copyright © 2009 John Wiley & Sons, Ltd.

Received 19 September 2008; Revised 2 February 2009; Accepted 3 February 2009

KEY WORDS: beam–columns; numerical integration; plastic hinges; sensitivity analysis

1. INTRODUCTION

Force-based frame finite elements have been shown to alleviate the need for mesh refinement in order to simulate the nonlinear material response of a beam–column structural member [1–3]. Owing to the structure of the governing equations of strong equilibrium and average compatibility, the integration method used in the state determination of force-based elements plays an important role in computing the element response. A variety of integration methods for force-based elements have been proposed in the literature over the past decade. Early implementations utilized Gauss–Lobatto quadrature [4] since it places sample points at the element ends where bending moments are largest in the absence of interior loads. The accuracy of Gauss–Lobatto quadrature ensures convergence of the element response under strain-hardening section response as the number of sample points increases; however, the high order of accuracy is rarely required in practical applications. Furthermore, as first pointed out in [5], the element response is not unique when deformations localize at a single integration point under strain-softening section response, thereby requiring modification of material properties in order to regularize the element response and maintain objectivity.

*Correspondence to: M. H. Scott, School of Civil and Construction Engineering, Oregon State University, 220 Owen Hall, Corvallis, OR 97331, U.S.A.
†E-mail: michael.scott@oregonstate.edu

Contract/grant sponsor: Oregon Department of Transportation (ODOT)

Subsequent developments [6, 7] introduced an analyst-specified plastic hinge length to the element state determination for regularization without modifying material properties. This allowed strain-softening element response to be regularized by a meaningful plastic hinge length rather than by that implied by the number of Gauss–Lobatto points. Despite the regularization of strain-softening response, these plastic hinge integration methods perform poorly for strain-hardening response and thus require *a priori* knowledge as to how the element will respond, which is not always clear, particularly for reinforced concrete members with variable axial loads. A regularized integration method that maintains numerical accuracy for strain-hardening behavior was subsequently developed [8] using interpolatory quadrature; however, it introduces additional parameters to standard integration rules and thus contributes to modeling uncertainty.

This paper develops analytic sensitivity by the direct differentiation method (DDM) for one-dimensional interpolatory quadrature, which is a generalization of most integration methods proposed for force-based frame elements. These developments allow modeling uncertainty associated with numerical integration in force-based elements to be assessed via stand-alone sensitivity analysis as well as part of gradient-based structural analyses such as reliability, optimization, and system identification. A brief overview of response sensitivity analysis is made, followed by direct differentiation of force-based element response using interpolatory quadrature. Numerical examples verify the analytic response sensitivity equations and demonstrate the effect of uncertain force-based element integration parameters in a reliability analysis.

2. OVERVIEW OF FINITE ELEMENT RESPONSE SENSITIVITY ANALYSIS

In accordance with the DDM [9], the first-order sensitivity of a structural system to changes in a parameter, θ, that represents an uncertain material, load, geometric, or integration property is determined by solution to the following system of equations:

$$\mathbf{K}_\mathrm{T}\frac{\partial \mathbf{U}}{\partial \theta} = \frac{\partial \mathbf{P}_f}{\partial \theta} - \left.\frac{\partial \mathbf{P}_\mathrm{r}}{\partial \theta}\right|_\mathbf{U} \tag{1}$$

where $\mathbf{K}_\mathrm{T}$ is the tangent stiffness matrix of the structure. The vector $\partial \mathbf{P}_f/\partial\theta$ represents the derivative of the applied loads with respect to the uncertain parameter, while $\partial \mathbf{P}_\mathrm{r}/\partial\theta|_\mathbf{U}$ is the conditional derivative of the resisting force vector, which is assembled from element contributions. The solution for $\partial \mathbf{U}/\partial\theta$ in Equation (1) gives the sensitivity of the nodal displacements to changes in the parameter, θ. The sensitivity of derived quantities such as member forces or plastic rotations can be obtained from $\partial \mathbf{U}/\partial\theta$ if desired. Extension to dynamic structural equilibrium is straightforward [10] and second-order derivatives of the structural response have been developed using the DDM [11].

3. FORCE-BASED FORMULATION WITH INTERPOLATORY QUADRATURE

In the force-based beam–column formulation [2], the element equilibrium relationship is stated in strong form as

$$\mathbf{s}(x) = \mathbf{b}(x)\mathbf{q} \tag{2}$$

where the matrix $\mathbf{b}$ contains interpolation functions that relate section forces, $\mathbf{s}$, along the element to basic forces, $\mathbf{q}$, at the element ends, as determined from static equilibrium of the basic system [12] shown in Figure 1. Without loss of generality, member loads are not included in Equation (2).

DOI: 10.1002/cnm

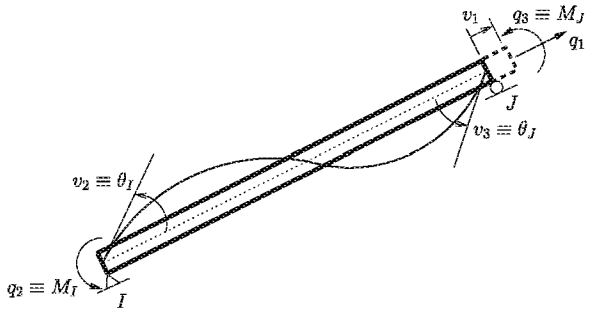

Figure 1. Basic system of element forces and deformations.

As a result, the section axial and shear forces are constant, while the section bending moment varies linearly along the element

$$\mathbf{b}(x) = \begin{bmatrix} 1 & 0 & 0 \\ 0 & x/L-1 & x/L \\ 0 & 1/L & 1/L \end{bmatrix} \tag{3}$$

From the principle of virtual forces, compatibility between section deformations, $\mathbf{e}$, and element deformations, $\mathbf{v}$, is satisfied in integral form and evaluated by numerical quadrature

$$\mathbf{v} = \sum_{i=1}^{N} \mathbf{b}^{\mathrm{T}}(x_i)\mathbf{e}(x_i)w_i \tag{4}$$

where x_i and w_i are the location and weight, respectively, of the ith integration point. In a finite element framework where the nodal displacements are the primary unknowns, force-based elements require an iterative state determination procedure to satisfy Equation (4) while maintaining equilibrium at each section along the element. An efficient procedure where residual element forces are propagated to the global system of equilibrium equations bypasses the need for iterations in the element state determination [3]. The variational basis for the force-based frame element state determination is described in [13, 14].

3.1. Interpolatory quadrature

Constructing integration methods via interpolatory quadrature [15] allows an analyst to control the location of sample points in force-based elements, which is advantageous for moving load analysis [16] and regularization [8]. For interpolatory quadrature, all the integration point locations are specified and the corresponding integration weights are obtained from the following system of Vandermonde equations:

$$\sum_{i=1}^{N} x_i^{j-1} w_i = \frac{L^j}{j} \quad (j = 1, \ldots, N) \tag{5}$$

where $[0, L]$ is the interval of integration.

In addition to specifying all integration point locations, it is possible to specify the integration weights at selected points, e.g. to correspond to prescribed plastic hinge lengths. These N_c weights and their associated sample points are denoted w_{ci} and x_{ci}, respectively. The $N_f = N - N_c$ remaining integration points and weights are denoted x_{fi} and w_{fi}. Splitting the summation in Equation (5) into separate sums over the N_c points with specified weights and the N_f points with unknown weights, then moving the known values to the right-hand side, leads to the following system of equations:

$$\sum_{i=1}^{N_f} x_{fi}^{j-1} w_{fi} = \frac{L^j}{j} - \sum_{i=1}^{N_c} x_{ci}^{j-1} w_{ci} \quad (j = 1, \ldots, N_f) \tag{6}$$

DOI: 10.1002/cnm

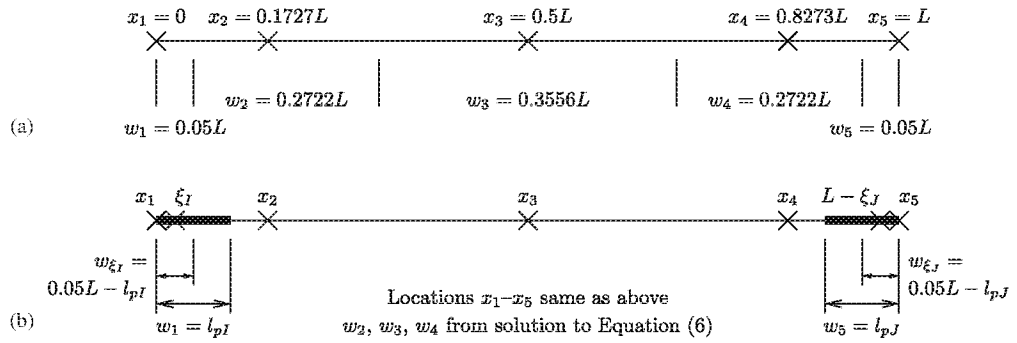

Figure 2. (a) Standard five-point Gauss–Lobatto integration rule and (b) five-point Gauss–Lobatto rule regularized by addition of two integration points just inside the element ends.

This reduced system of Vandermonde equations gives the remaining N_f weights required for evaluation of Equation (4).

3.2. Application to plastic hinge integration

The regularized integration method proposed in [8] demonstrates the application of the system of equations in Equation (6) to force-based elements. In this method, a standard quadrature rule is modified with two additional integration points placed at small distances, ξ_I and ξ_J, from the element ends, as shown in Figure 2(b). The weights of the integration points at the element ends equal to l_{pI} and l_{pJ}, while those just inside the element ends are based on the underlying quadrature rule, e.g. the five-point Gauss–Lobatto rule shown in Figure 2(a). This gives the following sets of locations and weights for use in Equation (6):

$$w_{ci} = \{l_{pI}, w_1 - l_{pI}, w_N - l_{pJ}, l_{pJ}\} \tag{7a}$$

$$x_{ci} = \{0, \xi_I, L - \xi_J, L\} \tag{7b}$$

$$x_{fi} = \{x_2, \ldots, x_{N-1}\} \tag{7c}$$

The remaining integration weights on the element interior are computed via Equation (6), which ensures integration accuracy in the linear-elastic range of response. Numerical stability of the underlying quadrature rule guarantees stability of the regularized integration with positive plastic hinge lengths [8], even when $l_{pI} > w_1$ and/or $l_{pJ} > w_N$, which leads to negative integration weights in Equation (7a). This integration method will be used in the numerical examples that conclude this paper; but first, the response sensitivity of interpolatory quadrature in force-based elements is developed.

4. RESPONSE SENSITIVITY ANALYSIS

Equivalent methods for analytic response sensitivity of force-based elements were developed in [17, 18] considering uncertain material parameters and many of the advantages of force-based frame elements over their displacement-based counterparts in simulating material nonlinear response are preserved in computing analytic response sensitivity [19]. Following the derivation in [17], the development of the response gradient begins by differentiation of the equilibrium relationship in Equation (2) taking into account variations in the basic and section force vectors and the force interpolation matrix

$$\frac{\partial \mathbf{s}}{\partial \theta} = \mathbf{b}\frac{\partial \mathbf{q}}{\partial \theta} + \frac{\partial \mathbf{b}}{\partial \theta}\mathbf{q} \tag{8}$$

DOI: 10.1002/cnm

where the derivative of the force interpolation matrix is

$$\frac{\partial \mathbf{b}}{\partial \theta} = \frac{1}{L}\begin{bmatrix} 0 & 0 & 0 \\ 0 & 1 & 1 \\ 0 & 0 & 0 \end{bmatrix} \frac{\partial x_i}{\partial \theta} \tag{9}$$

where $\partial x_i/\partial\theta$ is the derivative of the ith integration point location. In obtaining Equation (9), it is assumed the element length, L, is deterministic, i.e. that $\partial L/\partial\theta = 0$.

Differentiation of Equation (4) gives the derivative of the element deformations in terms of the derivatives of the section deformations, the force interpolation matrix, and the integration weights:

$$\frac{\partial \mathbf{v}}{\partial \theta} = \sum_{i=1}^{N} \left(\mathbf{b}^{\mathrm{T}} \frac{\partial \mathbf{e}}{\partial \theta} + \frac{\partial \mathbf{b}^{\mathrm{T}}}{\partial \theta} \mathbf{e} \right) w_i + \sum_{i=1}^{N} \mathbf{b}^{\mathrm{T}} \mathbf{e} \frac{\partial w_i}{\partial \theta} \tag{10}$$

After manipulation and combination of Equations (8) and (10) by a process identical to that outlined in [17], the conditional derivative of the basic forces is

$$\left.\frac{\partial \mathbf{q}}{\partial \theta}\right|_{\mathbf{v}} = \mathbf{k} \sum_{i=1}^{N} \mathbf{b}^{\mathrm{T}} \mathbf{f}_s \left(\left.\frac{\partial \mathbf{s}}{\partial \theta}\right|_{\mathbf{e}} - \frac{\partial \mathbf{b}}{\partial \theta} \mathbf{q} \right) w_i - \mathbf{k} \sum_{i=1}^{N} \left(\frac{\partial \mathbf{b}^{\mathrm{T}}}{\partial \theta} \mathbf{e} w_i + \mathbf{b}^{\mathrm{T}} \mathbf{e} \frac{\partial w_i}{\partial \theta} \right) \tag{11}$$

The term $\partial \mathbf{s}/\partial\theta|_{\mathbf{e}}$ represents the contribution of the section constitutive response to the element sensitivity, whereas the derivatives $\partial \mathbf{b}/\partial\theta$ and $\partial w_i/\partial\theta$ depend on the locations and weights of the element integration points, as described in the following section.

To evaluate the conditional derivative of the basic forces in Equation (11), it is necessary to differentiate Equation (6) with respect to θ, which may correspond to the location or weight of an integration point. Under the assumption that the interval of integration is held fixed, the sensitivity of the computed integration weights to θ is obtained by the differentiation of Equation (6) and the subsequent solution to the linear system of equations:

$$\sum_{i=1}^{N_f} x_{fi}^{j-1} \frac{\partial w_{fi}}{\partial \theta} = -\sum_{i=1}^{N_c} \left((j-1) x_{ci}^{j-2} \frac{\partial x_{ci}}{\partial \theta} w_{ci} + x_{ci}^{j-1} \frac{\partial w_{ci}}{\partial \theta} \right) - (j-1) \sum_{i=1}^{N_f} x_{fi}^{j-2} \frac{\partial x_{fi}}{\partial \theta} w_{fi} \tag{12}$$

For a single parameter, θ, at most one derivative on the right-hand side of Equation (12) will be non-zero. When θ corresponds to an integration point location, one of $\partial x_{ci}/\partial\theta$ or $\partial x_{fi}/\partial\theta$ will be equal to one and all other derivatives on the right-hand side of Equation (12) will be zero. Similarly, when θ corresponds to a specified integration weight, $\partial w_{ci}/\partial\theta$ will be equal to one while all other derivatives are equal to zero. The resulting solution of Equation (12) for $\partial w_{fi}/\partial\theta$ gives the sensitivity of the free integration weights to changes in the specified integration point locations and weights. These derivatives along with the binary values for the derivatives of w_{ci}, x_{ci}, and x_{fi} are incorporated in Equation (11) for subsequent calculation of the element response sensitivity to uncertain integration parameters. Since it is encapsulated within the element basic system, the incorporation of integration parameter uncertainty in large displacement response sensitivity analysis [20] is straightforward.

5. NUMERICAL EXAMPLES

Three examples, each involving the one degree indeterminate beam shown in Figure 3, demonstrate the essential features of analytic response sensitivity for interpolatory quadrature in force-based elements. The first example verifies that the sensitivity equations are correct via comparison with finite difference computations. This is followed by an example highlighting the differences in sensitivity to regularization parameters for strain-hardening and strain-softening behavior. The final example shows the efficiency of the analytic derivatives in a first-order reliability analysis, as well as demonstrating the importance of integration parameters on system reliability. The OpenSees finite element framework [21] serves as the environment for carrying out the examples.

DOI: 10.1002/cnm

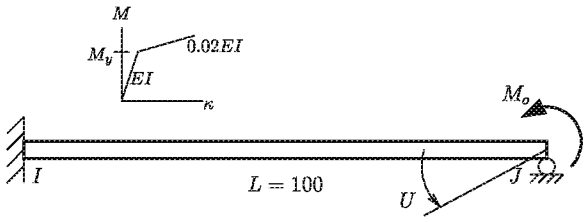

Figure 3. One degree indeterminate beam.

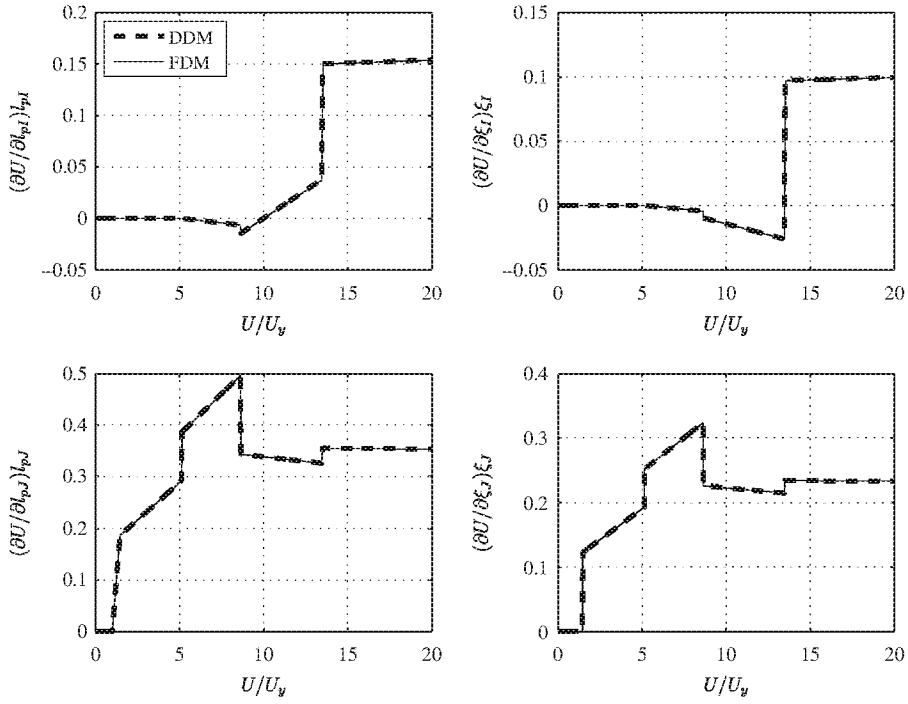

Figure 4. Sensitivity of end rotation to regularized integration parameters.

In each example, the five-point regularized Gauss–Lobatto integration shown in Figure 2(b) is applied in the element state determination with $l_{pI}=l_{pJ}=15.0$ and $\xi_I=\xi_J=1.0$. The moment–curvature response at each integration point is bilinear with $\alpha=2\%$ strain hardening. A concentrated moment is applied at the right end of the beam.

5.1. *Verification by finite differences*

The standard approach to verify DDM implementations is to compare the computed analytic derivatives with those obtained by finite difference computations. For decreasing parameter perturbations, the finite difference result should converge to that for the DDM

$$\lim_{\Delta\theta\to 0}\frac{R(\theta+\Delta\theta)-R(\theta)}{\Delta\theta}=\frac{\partial R}{\partial\theta} \tag{13}$$

DOI: 10.1002/cnm

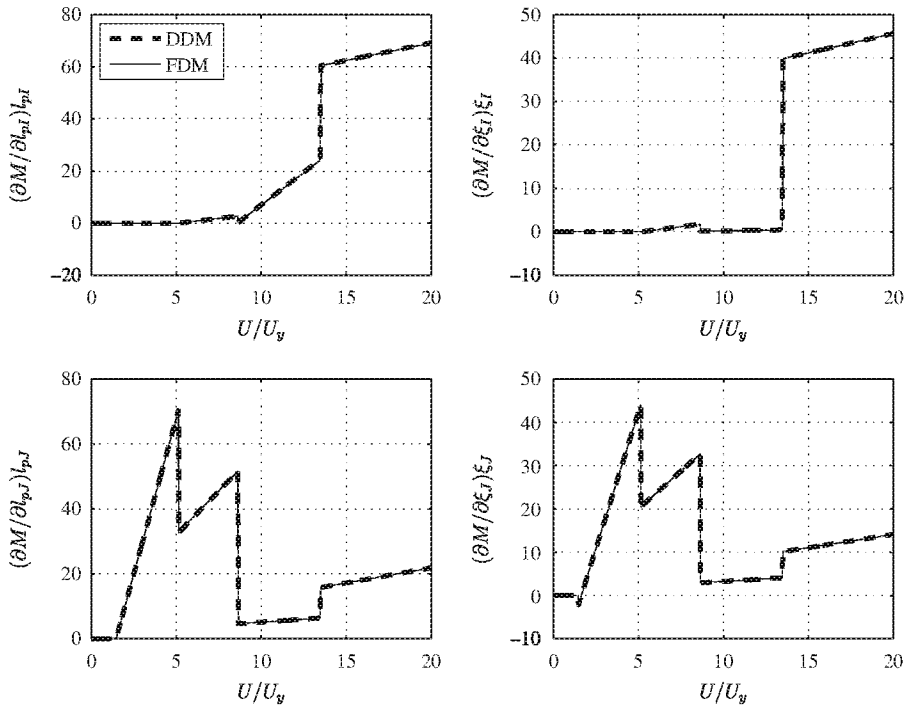

Figure 5. Sensitivity of reaction moment to regularized integration parameters.

where R is any response quantity of interest, e.g. nodal displacements, reactions, or internal forces/stresses.

The sensitivity of the end rotation, U, with respect to the four integration parameters (l_{pI}, l_{pJ}, ξ_I, and ξ_J) is shown in Figure 4 for monotonic increase in the applied moment to a rotation ductility (U normalized by yield value $U_y = M_y L/(4EI)$) of 20. As expected, there is zero sensitivity prior to yield at the free end of the beam. After yield, the sensitivity with respect to l_{pJ} and ξ_J becomes non-zero and continues to increase until the fixed end of the beam yields and the sensitivity with respect to l_{pI} and ξ_I becomes active. Discrete jumps in the response sensitivity occur as the constitutive model at each integration point switches from an elastic to yielding state [22]. The sensitivity of the internal bending moment at the fixed end of the beam [Figure 5] shows similar trends to that of the end rotation. In both cases, the DDM results match that obtained by finite differences with a perturbation of 0.01 times the nominal parameter value.

5.2. *Comparison of strain-hardening and strain-softening behavior*

With the DDM implementation verified, attention now turns to the difference in response sensitivity for strain-hardening and strain-softening moment–curvature response of the beam. For strain-hardening response, plasticity spreads along the beam; however, deformations localize at a single section under strain-softening response, causing the remaining portions of the beam to unload in order to maintain equilibrium.

The calculation of response sensitivity confirms that the plastic hinge length associated with the section where localization occurs controls the beam response under strain-softening behavior. As shown in Figure 6, the sensitivity of the end rotation to l_{pJ} increases indefinitely for strain-softening behavior as compared with that of strain hardening, which remains relatively low as yielding is able to spread across the beam and activate the sensitivity to other constitutive and integration parameters. While the results of this example are obvious, they demonstrate that the element response sensitivity follows the expected behavior under strain-softening constitutive behavior and provide further verification of the implementation.

DOI: 10.1002/cnm

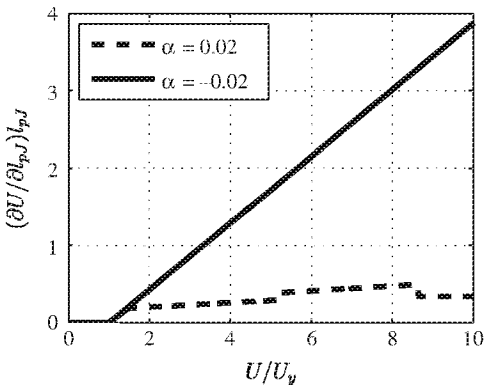

Figure 6. Comparison of end rotation sensitivity to plastic hinge length for strain-hardening and strain-softening behavior.

Table I. Random variable distributions assigned to the uncertain parameters in reliability analysis and their values and importance measures at most probable failure point (MPP).

Parameter	Distribution	COV	Mean	Correlation	MPP	Importance
Plastic hinge length, l_{pI}	Normal	0.2	15.0	0.3	15.71	0.00039
Plastic hinge length, l_{pJ}					17.36	0.2275
Distance, ξ_I	Normal	0.2	1.0	0.3	1.005	−0.00178
Distance, ξ_J					1.020	0.02947
Yield moment @ $x=0$	Lognormal	0.1	1000.0	0.7	943.1	−0.1632
Yield moment @ $x=\xi_I$					960.2	0
Yield moment @ $x=L-\xi_J$	Lognormal	0.1	1000.0	0.7	1001.0	0.5519
Yield moment @ $x=L$					860.6	−0.7850

5.3. *First-order reliability analysis*

To assess the importance of the integration parameters relative to common sources of aleatory uncertainty, a first-order reliability (FORM) analysis is conducted in this example. The distribution, mean value, and coefficient of variation for each random variable are shown in Table I. The plastic hinge lengths and integration parameters are each treated as pairs of correlated normal random variables, while the section yield moments at the corresponding locations are modeled as lognormal random variables with strong correlation at each end of the beam. To reflect the large amount of uncertainty in representing plastic hinge formation, the coefficient of variation for integration parameters is assigned a larger value than that of the section yield moment.

The performance function defines failure as the end rotation ductility exceeding 15 at a load of $M_o = 1500$.

$$g = 15U_y - U \tag{14}$$

At the mean values of the random variables, the computed end rotation ductility is 10 at the specified load level. Thus, the performance function defines failure as the end rotation exceeding its nominal value by 50%. Using the HLRF algorithm with Armijo step size reduction [23], the solution point is found in eight iteration at a reliability index of $\beta = 2.193$, which corresponds to a 1.43% probability of failure.

The parameter values at the most probable failure point are shown in Table I, along with importance measures that account for the prescribed correlation between the random variables (γ-values [24]). The importance measures show that the yield moments at the free end of the beam have the most influence on the response at the failure point, followed by the yield moment at the beam's fixed end. Of the four integration parameters, the plastic hinge length at the free end, l_{pJ}, ranks highest in importance, while the others have relatively low

DOI: 10.1002/cnm

importance. This quantification of uncertainty confirms the expected result that the integration parameters for the sections with the largest bending moment have the highest relative ranking.

Using analytic gradients (DDM) of the performance function to determine search directions, the FORM analysis requires 22 function evaluations to reach the solution point. On the other hand, gradients computed by finite differences require 94 function evaluations in order to converge to the same solution. Although this is a small problem for which computational cost is negligible, the reduction in function evaluations indicates that the potential for significant computational savings in the finite element reliability analysis of larger systems where parameters such as plastic hinge lengths are treated as uncertain random variables.

6. CONCLUSIONS

Equations have been derived, via direct differentiation of interpolatory quadrature, for the analytic sensitivity of force-based beam finite element response with respect to the locations and weights of integration points. Finite difference computations verify the implementation of the analytic sensitivity equations is correct and a first-order reliability analysis demonstrates that fewer-limit state function evaluations are required when using analytic gradients in the search for the most probable point of failure. For the reliability example presented, rankings show that plastic hinge lengths rank high in importance, on par with material constitutive parameters, while the parameters corresponding to integration point locations rank relatively low. It is anticipated that integration point locations would rank higher in importance for the reliability analysis of frames with large strain $P-\delta$ effects [25], and this is an area of future research. At any rate, the developments of this paper allow the epistemic uncertainty of selecting a force-based integration method to be quantified, as well as permitting integration points and weights to be treated as random variables in a probabilistic structural analysis.

ACKNOWLEDGEMENTS

The application of interpolatory quadrature to force-based elements was a derivative of research sponsored by the Oregon Department of Transportation (ODOT) into efficient methods of load rating bridge girders. The authors are thankful for the support provided by ODOT; however, the views expressed in this paper do not necessarily reflect those of the sponsor.

REFERENCES

1. Ciampi V, Carlesimo L. A nonlinear beam element for seismic analysis of structures. *The 8th European Conference on Earthquake Engineering*. Lisbon, Portugal, 1986.
2. Spacone E, Ciampi V, Filippou FC. Mixed formulation of nonlinear beam finite element. *Computers and Structures* 1996; **58**(1):71–83.
3. Neuenhofer A, Filippou FC. Evaluation of nonlinear frame finite-element models. *Journal of Structural Engineering* 1997; **123**(7):958–966.
4. Abramowitz M, Stegun CA (eds). *Handbook of Mathematical Functions with Formulas, Graphs, and Mathematical Tables* (9th edn). Dover: New York, NY, 1972.
5. Coleman J, Spacone E. Localization issues in force-based frame elements. *Journal of Structural Engineering* 2001; **127**(11):1257–1265.
6. Scott MH, Fenves GL. Plastic hinge integration methods for force-based beam–column elements. *Journal of Structural Engineering* 2006; **132**(2):244–252.
7. Addessi D, Ciampi V. A regularized force-based beam element with a damage-plastic section constitutive law. *International Journal for Numerical Methods in Engineering* 2007; **70**(5):610–629.
8. Scott MH, Hamutçuoğlu O. Numerically consistent regularization of force-based frame elements. *International Journal for Numerical Methods in Engineering* 2008; **76**(10):1612–1631.
9. Kleiber M, Antunez H, Hien TD, Kowalczyk P. *Parameter Sensitivity in Nonlinear Mechanics*. Wiley: New York, 1997.
10. Franchin P. Reliability of uncertain inelastic structures under earthquake excitation. *Journal of Engineering Mechanics* 2004; **130**(2):180–191.

DOI: 10.1002/cnm

11. Bebamzadeh A, Haukaas T. Second-order sensitivities of inelastic finite-element response by direct differentiation. *Journal of Engineering Mechanics* 2008; **134**(10):867–880.
12. Crisfield MA. *Non-linear Finite Element Analysis of Solids and Structures*, vol. 1. Wiley: New York, 1991.
13. Hjelmstad KD, Taciroglu E. Mixed variational methods for finite element analysis of geometrically non-linear, inelastic Bernoulli–Euler beams. *Communications in Numerical Methods in Engineering* 2003; **19**(10):809–832.
14. Hjelmstad KD, Taciroglu E. Variational basis of nonlinear flexibility methods for structural analysis of frames. *Journal of Engineering Mechanics* 2005; **131**(11):1157–1169.
15. Golub GH, Van Loan CF. *Matrix Computations* (3rd edn). Johns Hopkins University Press: Baltimore, MD, 1996.
16. Kidarsa A, Scott MH, Higgins CC. Analysis of moving loads using force-based finite elements. *Finite Elements in Analysis and Design* 2008; **44**(4):214–224.
17. Scott MH, Franchin P, Fenves GL, Filippou FC. Response sensitivity for nonlinear beam–column elements. *Journal of Structural Engineering* 2004; **130**(9):1281–1288.
18. Conte JP, Barbato M, Spacone E. Finite element response sensitivity analysis using force-based frame models. *International Journal for Numerical Methods in Engineering* 2004; **59**:1781–1820.
19. Barbato M, Conte JP. Finite element response sensitivity analysis: a comparison between force-based and displacement-based frame element models. *Computer Methods in Applied Mechanics and Engineering* 2005; **194**:1479–1512.
20. Scott MH, Filippou FC. Exact response gradients for large displacement nonlinear beam–column elements. *Journal of Structural Engineering* 2007; **133**(2):155–165.
21. McKenna F, Fenves GL, Scott MH. *Open System for Earthquake Engineering Simulation*. University of California: Berkeley, CA, 2000. Available from: http://opensees.berkeley.edu.
22. Conte JP, Vijalapura PK, Meghella M. Consistent finite-element response sensitivity analysis. *Journal of Engineering Mechanics* 2003; **129**(12):1380–1393.
23. Haukaas T, Der Kiureghian A. Strategies for finding the design point in non-linear finite element reliability analysis. *Probabilistic Engineering Mechanics* 2006; **21**(2):133–147.
24. Haukaas T, Der Kiureghian A. Parameter sensitivity and importance measures in nonlinear finite element reliability analysis. *Journal of Engineering Mechanics* 2005; **131**(10):1013–1026.
25. De Souza RM. Force-based finite element for large displacement inelastic analsysis of frames. *Ph.D. Thesis*, University of California, Berkeley, CA, 2000.

DOI: 10.1002/cnm